

# Journal of Materials Chemistry A

Accepted Manuscript



This is an *Accepted Manuscript*, which has been through the Royal Society of Chemistry peer review process and has been accepted for publication.

*Accepted Manuscripts* are published online shortly after acceptance, before technical editing, formatting and proof reading. Using this free service, authors can make their results available to the community, in citable form, before we publish the edited article. We will replace this *Accepted Manuscript* with the edited and formatted *Advance Article* as soon as it is available.

You can find more information about *Accepted Manuscripts* in the [Information for Authors](#).

Please note that technical editing may introduce minor changes to the text and/or graphics, which may alter content. The journal's standard [Terms & Conditions](#) and the [Ethical guidelines](#) still apply. In no event shall the Royal Society of Chemistry be held responsible for any errors or omissions in this *Accepted Manuscript* or any consequences arising from the use of any information it contains.

## Hybrid Lead iodide perovskite and Lead sulfide QDs heterojunction solar cell to Obtain Panchromatic Response

Lioz Etgar<sup>1,\*</sup>, Peng Gao<sup>2</sup>, Peng Qin<sup>2</sup>, Michael Gratzel<sup>2</sup> and Mohammad Khaja Nazeeruddin<sup>\*2</sup>

<sup>1</sup> Institute of Chemistry, The Hebrew University of Jerusalem, Jerusalem 91904, Israel

<sup>2</sup> Laboratoire de Photonique et Interfaces, Institut des Sciences et Ingénierie Chimiques, École Polytechnique Fédérale de Lausanne (EPFL), Switzerland. [Lioz.etgar@mail.huji.ac.il](mailto:Lioz.etgar@mail.huji.ac.il); [mdkhajanazeeruddin@epfl.ch](mailto:mdkhajanazeeruddin@epfl.ch)

We report for the first time on co-sensitization between  $\text{CH}_3\text{NH}_3\text{PbI}_3$  perovskite and PbS quantum dots (QDs) in a heterojunction solar cell to obtain panchromatic response from the visible to near IR regions. Following the sensitizers deposition on  $\text{TiO}_2$  film, an Au thin layer is evaporated on top as a back contact. Importantly, the  $\text{CH}_3\text{NH}_3\text{PbI}_3$  nanoparticles and the PbS QDs assume here simultaneously both the role of light harvester and hole conductor, rendering superfluous the use of an additional hole transporting material. The mesoscopic  $\text{CH}_3\text{NH}_3\text{PbI}_3$  (perovskite) – PbS (QDs) / $\text{TiO}_2$  heterojunction solar cell shows impressive short circuit photocurrent ( $J_{sc}$ ) of  $24.63 \text{ mA/cm}^2$ , much higher than the individual  $\text{CH}_3\text{NH}_3\text{PbI}_3$  perovskite and the PbS QDs solar cells. The advent of such co-sensitization mesoscopic heterojunction solar cells paves the way to extend the absorbance region of the promising low cost, high-efficiency perovskite based solar cells.

### Introduction

The hybrid organic-inorganic methylammonium lead halide perovskites ( $\text{CH}_3\text{NH}_3\text{PbX}_3$ ,  $\text{X} = \text{Cl}^-, \text{Br}^-, \text{I}^-$ ) pioneered by Mitzi, et.al.<sup>[1]</sup> and introduced as a light harvester in dye sensitized solar cell configurations by Miyazaka et.al.<sup>[2]</sup> have attracted intensive attention for thin-film photovoltaics. The advantages of hybrid organic-inorganic methylammonium lead halide perovskite are large absorption coefficient, high charge carrier mobility and diffusion lengths<sup>[3-10]</sup>. Using methylammonium lead iodide perovskite as a light harvester, and 2,2',7,7'-tetrakis(N,N-di-p-methoxyphenylamine) - 9,9'-spirobifluorene (spiro-MeOTAD) as an hole transporting material, power conversion efficiencies (PCEs) of over 16% were obtained with both mesoporous metal oxide scaffold and in planar heterojunction architectures<sup>[11,12,13,14]</sup> The ease with which these organic-inorganic hybrid perovskite materials can be prepared and processed from

solution<sup>[3-13]</sup> whilst simultaneously providing desired device characteristics have made them an attractive alternative for thin film photovoltaics. Lee *et al.*<sup>[4]</sup> showed that a mixed-halide perovskite on a mesoporous Al<sub>2</sub>O<sub>3</sub> photoanode acts both as light absorber and electron conductor, others, and we have shown that the pure iodide perovskite can act as a hole conductor.<sup>[7],[15]</sup> This demonstrates the interesting properties of perovskites in that they do not only act as light absorbers but participate in the charge conduction.

However, the absorption onset of the CH<sub>3</sub>NH<sub>3</sub>PbI<sub>3</sub> perovskite is limited to 1.57 eV. Therefore, an effective approach to further increase the spectral response of these materials is co-sensitization with near IR absorbing nanoparticles. In the Co-sensitization approach a combination of two or more sensitized materials are absorbing the light.

Near IR Quantum Dots (QDs) have been used in several solar cells architectures such as QD-Schottky barrier solar cells, QD-polymer hybrid solar cells, QD-sensitized titanium dioxide (TiO<sub>2</sub>) solar cells, and QD hybrid bilayer solar cells.<sup>[16-25]</sup> Efficiencies of 5-7% were achieved.<sup>[26-35]</sup>

Here we report for the first time on the co-sensitization between organo lead-halide perovskite and PbS QDs in a heterojunction solar cell. In this unique structure both the perovskite and the QDs used as sensitizers and at the same time as hole conductors. The function of each material separately as sensitizer and at the same time as hole conductor in heterojunction solar cell was already proved in previous reports.<sup>[7],[15]</sup> The J<sub>SC</sub> of the co-sensitized devices were significantly enhanced relative to their corresponding single-sensitized devices, improving the overall performance for the CH<sub>3</sub>NH<sub>3</sub>PbI<sub>3</sub> perovskite + PbS QDs device by 18% with respect to the CH<sub>3</sub>NH<sub>3</sub>PbI<sub>3</sub> devices.

## Results and Discussion

Figure 1A, shows a scheme of the co-sensitization of CH<sub>3</sub>NH<sub>3</sub>PbI<sub>3</sub> with the PbS QDs on a 500nm TiO<sub>2</sub> film. The PbS QDs used in this study were with their original ligands oleic acid, they had 1<sup>st</sup> excitonic peak at 920nm wavelength corresponding to E<sub>g</sub> of 1.38eV. The synthesis of CH<sub>3</sub>NH<sub>3</sub>PbI<sub>3</sub> and deposition on the mesoporous TiO<sub>2</sub> film was carried out by spin coating of a 40 wt% precursor solution of CH<sub>3</sub>NH<sub>3</sub>I and PbI<sub>2</sub> in  $\gamma$ -butyrolactone. Upon drying at room temperature the film coated onto the TiO<sub>2</sub> darkened in color, indicating the formation of CH<sub>3</sub>NH<sub>3</sub>PbI<sub>3</sub> in the solid state. The ionic and covalent interaction between the metal cations and the halogen anions creates inorganic octahedra, while the cationic alkylammonium head groups provide charge balance to the

structure.

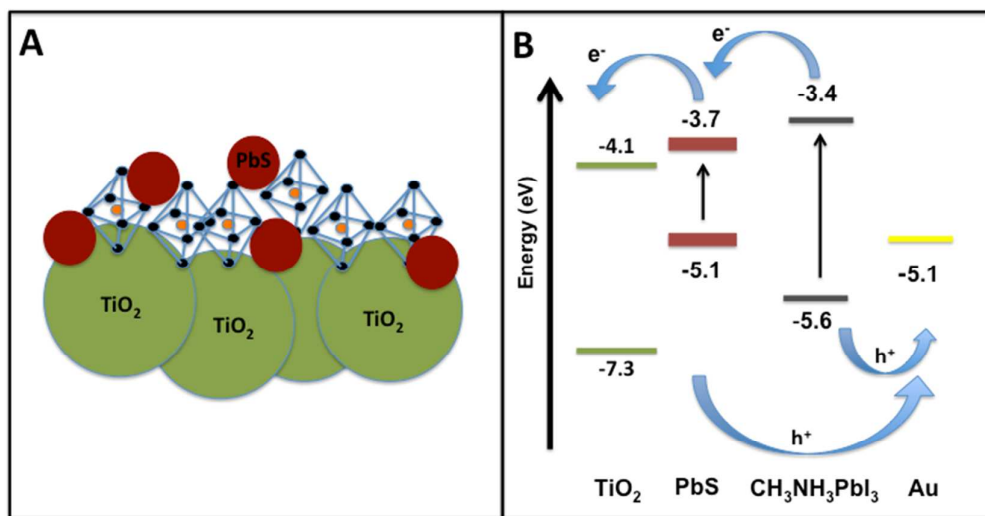


**Figure 1:** (A) Schematic presentation of the hybrid perovskite – PbS QDs heterojunction solar cell. (B) Energy level diagram of the components involved in the cell.

The CH<sub>3</sub>NH<sub>3</sub>PbI<sub>3</sub>, coated TiO<sub>2</sub> electrode was then deposited the PbS QDs using spin-coating method. Finally a gold was evaporated as the back contact of the device. Figure 1B shows a schematic energy level diagram of the hybrid CH<sub>3</sub>NH<sub>3</sub>PbI<sub>3</sub> - PbS QDs heterojunction solar cell. Upon illumination the CH<sub>3</sub>NH<sub>3</sub>PbI<sub>3</sub> perovskite and the PbS QDs absorbs the light, as a result electrons can go in three possible channels, (i) electron injection from the CH<sub>3</sub>NH<sub>3</sub>PbI<sub>3</sub> perovskite to the TiO<sub>2</sub> (ii) electron injection from the PbS QDs to the TiO<sub>2</sub> and (iii) an electron transfer from the CH<sub>3</sub>NH<sub>3</sub>PbI<sub>3</sub> perovskite to the PbS QDs. Figure 2A shows the absorption spectra of the CH<sub>3</sub>NH<sub>3</sub>PbI<sub>3</sub> perovskite and the PbS QDs on TiO<sub>2</sub> films, and the co-sensitization absorption spectra of the CH<sub>3</sub>NH<sub>3</sub>PbI<sub>3</sub> perovskite + 3 layers of PbS QDs. The PbS QDs have an absorption in the NIR region, while the absorption of the CH<sub>3</sub>NH<sub>3</sub>PbI<sub>3</sub> goes only till 800nm wavelength. The absorption of the co-sensitization system shows both contributions from the CH<sub>3</sub>NH<sub>3</sub>PbI<sub>3</sub> and the PbS QDs.

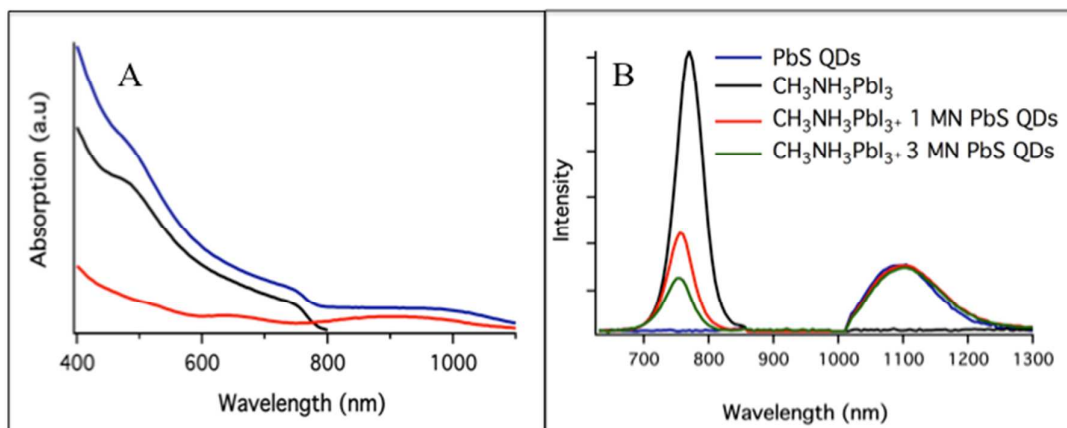


**Figure 2:** (A) Absorption spectra on TiO<sub>2</sub> NPs film of the PbS QDs, Lead iodide perovskite and Lead iodide perovskite with 3 layers of PbS QDs. (B) Emission spectra of the PbS QDs, Lead iodide perovskite and Lead iodide perovskite with 3 layers of PbS QDs.

Further proof for the light harvesting contribution from both sensitizers can be observed in the emission spectra shown in figure 2B. All measurements were done on ZrO<sub>2</sub> substrate in order to use similar morphology as the TiO<sub>2</sub> and at the same time to make sure that no injection of electrons will occur. In the case of the PbS QDs the emission peak can be recognized around 1100nm, for the CH<sub>3</sub>NH<sub>3</sub>PbI<sub>3</sub> perovskite the emission peak can be observed around 760nm. In the case of the hybrid CH<sub>3</sub>NH<sub>3</sub>PbI<sub>3</sub> perovskite + 3 layers of PbS QDs both emission peaks can be seen clearly which suggest the activity of both materials in the hybrid structure. Interestingly, quenching of the emission spectra at 760nm wavelength can be observed when adding the PbS QDs layers. On the other hand the emission at 1100nm wavelength, which belongs to the PbS QDs, isn't decreasing, suggesting energy transfer from perovskite to PbS QDs.

In order to find the best co-sensitization system we tried different number of QDs layers deposition on top of the perovskite. The photovoltaic parameters, for the CH<sub>3</sub>NH<sub>3</sub>PbI<sub>3</sub> perovskite + different number of layers of PbS QDs (the co-sensitized devices) and that of either individual PbS QDs or CH<sub>3</sub>NH<sub>3</sub>PbI<sub>3</sub> perovskite device are summarized in Table 1. The results show clearly that the best photovoltaic performance was achieved upon co-sensitization with the system composed of CH<sub>3</sub>NH<sub>3</sub>PbI<sub>3</sub> perovskite + 3 layers of PbS QDs. The performance of the CH<sub>3</sub>NH<sub>3</sub>PbI<sub>3</sub> perovskite + 3 layers of PbS QDs device improved mainly due to the enhancement in the current density to yield 24.63 mA/cm<sup>2</sup>. In

the case of 1 layer of PbS QDs almost no contribution in the Near Infra-Red (NIR) region from the PbS QDs occurs, therefore small enhancement in the  $J_{sc}$  observed, when 6 layers of PbS QDs were deposited some of the perovskite was removed from the surface which affected the  $J_{sc}$  of the device, finally the deposition of 3 layers of PbS QDs on the perovskite results in the best photovoltaic performance. The main advantage in co-sensitization is to extend the absorption region of the solar cell, in this study the hybrid perovskite-QDs structure has an additional advantage. The inorganic halides atoms in the  $\text{CH}_3\text{NH}_3\text{PbI}_3$  perovskite could remove the dangling bonds caused by the excess Pb at the surface of the PbS QDs and in addition passivate the surface states of the QDs. These results with better stability and suppress surface trapping of the PbS QDs.

**Table 1:** Summary of the photovoltaic parameters for the different cells.

Cell type	$J_{sc}$ (mA/cm <sup>2</sup> )	Voc (mV)	FF	$\eta$ (%)
$\text{CH}_3\text{NH}_3\text{PbI}_3$	8.33	665.3	0.55	3.04
$\text{CH}_3\text{NH}_3\text{PbI}_3$ +1 layer PbS QDs	8.6	471	0.5	2.06
$\text{CH}_3\text{NH}_3\text{PbI}_3$ +3 layers PbS QDs	24.63	343.8	0.43	3.6
$\text{CH}_3\text{NH}_3\text{PbI}_3$ +6 layers PbS QDs	11	588.8	0.47	2.9
3 layers PbS QDs	0.077	211	0.29	0.004

The current–voltage characteristics and the corresponding IPCE spectra are shown in figure 3A and 3B, respectively. For the co-sensitized system, the enhancement of  $J_{sc}$  is understandable from the IPCE spectra; the contribution of the PbS QDs to the NIR region can be observed in addition to the enhancement in the visible region where both materials absorb light. As a result,  $J_{sc}$  of the co-sensitized device increased from 8.33 mA cm<sup>-2</sup> to 24.63 mA cm<sup>-2</sup> to contribute three times enhancement of the current and 18% overall performance. From the current-voltage and EQE spectra, we can infer that the PbS/ $\text{CH}_3\text{NH}_3\text{PbI}_3$ /mp-TiO<sub>2</sub> solar cell device delivering photovoltaic response from both the materials. The enhanced device efficiency is attributed to the charge injection

occurring from both the sensitizers and to some extent possible energy transfer from high energy perovskite to the lower energy PbS QD's. What is astonishing is  $24.63 \text{ mA}\cdot\text{cm}^{-2}$  extracted current demonstrating charge collection efficiency of these materials. The open circuit potential and the fill factor are low, which we are optimizing by using different linker molecules to adsorb PbS QD's.

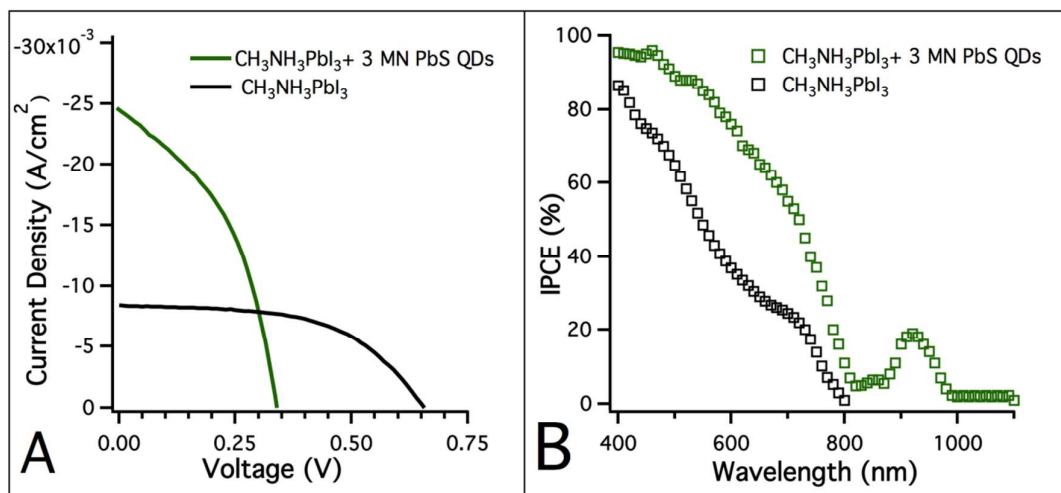


**Figure 3:** J-V measurements of the Lead iodide perovskite heterojunction solar cell and the hybrid PbS QDs Lead iodide perovskite heterojunction solar cell. (B) The IPCE of the same heterojunction solar cells.

## Conclusions

This work reports for the first time on co-sensitization between lead iodide perovskite and PbS QDs in heterojunction solar cell. As a result of this co-sensitization the photocurrent density increased, achieving more than  $24 \text{ mA}/\text{cm}^2$ . The co-sensitization opens the possibility to advent the high absorption of the perovskite in the visible region and to have the NIR contribution of the PbS QDs. The fact that the individual perovskite solar cell already demonstrated high efficiency (using its visible absorption spectra) opens up new avenues for future development of high efficiency photovoltaic cells when increasing the Voc and FF through control of the binding between the two sensitizers could result power conversion efficiency as high as 18%.

## Experimental

### Method and device fabrication

**Colloidal PbS QDs** capped with oleic acid were purchased from Evident technologies and stored in nitrogen-filled glove box.

**CH<sub>3</sub>NH<sub>3</sub>I** was synthesized by reacting 30 mL methylamine (40% in methanol, TCI) and 32.3 mL of hydroiodic acid (57 wt% in water, Aldrich) in a 250 mL round bottomed flask at 0 °C for 2 h with stirring. The precipitate was recovered by putting the solution on a rotavap and carefully removing the solvents at 50 °C. The yellowish raw product of methylammonium iodide (CH<sub>3</sub>NH<sub>3</sub>I), was washed with diethyl ether by stirring the solution for 30 min, a step which was repeated three times, and then finally recrystallized from a mixed solvent of diethyl ether and ethanol. After filtration, the solid was collected and dried at 60 °C in vacuum oven for 24 h.

**Device fabrication** - Thin dense TiO<sub>2</sub> layers of ~100 nm thickness were deposited onto a SnO<sub>2</sub>:F conducting glass substrate (15Ω/cm, Pilkington) by the spray pyrolysis method.<sup>36</sup> The deposition temperature of the TiO<sub>2</sub> compact layer was 450 °C. TiO<sub>2</sub> nanoparticles films of ~ 0.5 μm thickness were spin-coated onto this substrate. The TiO<sub>2</sub> layer was annealed at 500 °C for 30 min in air. The substrate was immersed in 40 mM TiCl<sub>4</sub> aqueous solutions for 30 min at 70 °C and washed with distilled water and ethanol, followed by annealing at 500 °C for 30 min in air.

The synthesis of CH<sub>3</sub>NH<sub>3</sub>PbI<sub>3</sub> on the TiO<sub>2</sub> surface was carried out by dropping a 40 wt% precursor solution of equimolar CH<sub>3</sub>NH<sub>3</sub>I and PbI<sub>2</sub> in γ-butyrolactone onto the TiO<sub>2</sub> film. Film formation was induced by spin coating (2000 rpm, 30 sec) under glove box conditions. The film coated on the TiO<sub>2</sub> changed color upon drying at room temperature, indicating the formation of CH<sub>3</sub>NH<sub>3</sub>PbI<sub>3</sub> in the solid state. The CH<sub>3</sub>NH<sub>3</sub>PbI<sub>3</sub> film was annealed under argon for 15min at 100°C.

Following the CH<sub>3</sub>NH<sub>3</sub>PbI<sub>3</sub> film deposition, PbS QDs with their original ligands (oleic acid) were deposited by spin coating on top of the CH<sub>3</sub>NH<sub>3</sub>PbI<sub>3</sub> perovskite.

Finally the counter electrode was deposited by thermal evaporation of gold under a pressure of 5×10<sup>-5</sup> Torr. The active area was 0.12 cm<sup>2</sup>. After the preparation, the cells were allowed to be exposed to air.

#### Photovoltaic Characterization

Photovoltaic measurements employed an AM 1.5 solar simulator equipped with a 450W xenon lamp (Model No. 81172, Oriel). Its power output was adjusted to match AM 1.5 global sunlight (100 mW/cm<sup>2</sup>) by using a reference Si photodiode equipped with an IR-



cutoff filter (KG-3, Schott) in order to reduce the mismatch between the simulated light and AM 1.5 (in the region of 350–750 nm) to less than 2% with measurements verified at two PV calibration laboratories [ISE (Germany), NREL (USA)]. I–V curves were obtained by applying an external bias to the cell and measuring the generated photocurrent with a Keithley model 2400 digital source meter. The voltage step and delay time of photocurrent were 10 mV and 40 ms, respectively. A similar data acquisition system was used to determine the monochromatic incident photon- to-electric current conversion efficiency. Under full computer control, light from a 300 W xenon lamp (ILC Technology, U.S.A.) was focused through a Gemini-180 double monochromator (Jobin Yvon Ltd., U.K.) onto the photovoltaic cell under test. The monochromator was incremented through the visible spectrum to generate the IPCE ( $\lambda$ ) as defined by IPCE ( $\lambda$ ) =  $12400(J_{sc}/\lambda\phi)$ , where  $\lambda$  is the wavelength,  $J_{sc}$  is short-circuit photocurrent density ( $\text{mA cm}^{-2}$ ), and  $\phi$  is the incident radiative flux ( $\text{mW cm}^{-2}$ ). Photovoltaic performance was measured by using a metal mask with an aperture area of  $0.12 \text{ cm}^2$ . The measurements were performed under bias light.

## References

- [1] S. Wang, D. B. Mitzi, C. A. Feild, A. Guloy, *J. Am. Chem. Soc.* **1995**, *117*, 5297.
- [2] A. Kojima, K. Teshima, Y. Shirai, T. Miyasaka, *J. Am. Chem. Soc.* **2009**, *131*, 6050.
- [3] J. Im, C. Lee, J. Lee, S. Park, N. Park, *Nanoscale* **2011**, *3*, 4088.
- [4] M. M. Lee, J. Teuscher, T. Miyasaka, T. N. Murakami, H. J. Snaith, *Science* **2012**, *338*, 643.
- [5] J. Im, J. Chung, S.-J. Kim, N. Park, *Nanoscale Res. Lett.* **2012**, *7*, 353.
- [6] H.-S. Kim, C.-R. Lee, J.-H. Im, K.-B. Lee, T. Moehl, A. Marchioro, S.-J. Moon, R. Humphry-Baker, J.-H. Yum, J. E. Moser, M. Grätzel, N.-G. Park, *Sci. Rep.* **2012**, *2*, 591.
- [7] L. Etgar, P. Gao, Z. Xue, Q. Peng, A. K. Chandiran, B. Liu, M. K. Nazeeruddin, M. Grätzel, M. Grätzel, M. Grätzel, *J. Am. Chem. Soc.* **2012**, *134*, 17396.
- [8] G. E. Eperon, V. M. Burlakov, P. Docampo, A. Goriely, H. J. Snaith, *Adv. Funct. Mater.* **2014**, *24*, 151.
- [9] P. Qin, A. L. Domanski, A. K. Chandiran, R. Berger, H.-J. Butt, M. I. Dar, T. Moehl, N. Tetreault, P. Gao, S. Ahmad, M. K. Nazeeruddin, M. Grätzel, *Nanoscale*. **2014**, *6*, 1508..
- [10] M. J. Carnie, C. Charbonneau, M. L. Davies, J. Troughton, T. M. Watson, K. Wojciechowski, H. Snaith, D. A. Worsley, *Chem. Commun. (Camb)*. **2013**, *49*, 7893.
- [11] S. Ryu, J. H. Noh, N. J. Jeon, Y. C. Kim, W. S. Yang, J. W. Seo, and S. Il Seok, *Energy Environ. Sci.*, **2014**, 10.1039/c4ee00762j.
- [12] N. J. Jeon, H. G. Lee, Y. C. Kim, J. Seo, J. H. Noh, J. Lee, and S. Il Seok, *J. Am. Chem. Soc.*, **2014**, 10.1021/ja502824c.
- [13] J. Burschka, N. Pellet, S.-J. Moon, R. Humphry-Baker, P. Gao, M. K. Nazeeruddin, M. Grätzel, *Nature* **2013**, *499*, 316.
- [14] M. Liu, M. B. Johnston, H. J. Snaith, *Nature* **2013**, *501*, 395.

- 
- [15] W. A. Laban, L. Etgar, *Energy Environ. Sci.* **2013**, *6*, 3249.
- [16] J. M. Luther, M. Law, M. C. Beard, Q. Song, M. O. Reese, R. J. Ellingson, A. J. Nozik, *Nano Lett.* **2008**, *8*, 3488.
- [17] W. Ma, J. M. Luther, H. Zheng, Y. Wu, A. P. Alivisatos, *Nano Lett.* **2009**, *9*, 1699.
- [18] R. Plass, S. Pelet, J. Krueger, M. Grätzel, U. Bach, *J. Phys. Chem. B* **2002**, *106*, 7578.
- [19] B. Sun, A. T. Findikoglu, M. Sykora, D. J. Werder, V. I. Klimov, *Nano Lett.* **2009**, *9*, 1235.
- [20] J. M. Luther, M. Law, Q. Song, C. L. Perkins, M. C. Beard, A. J. Nozik, *ACS Nano* **2008**, *2*, 271.
- [21] S. Zhang, P. W. Cyr, S. A. McDonald, G. Konstantatos, E. H. Sargent, *Appl. Phys. Lett.* **2005**, *87*, 233101.
- [22] B.-R. Hyun, Y.-W. Zhong, A. C. Bartnik, L. Sun, H. D. Abruña, F. W. Wise, J. D. Goodreau, J. R. Matthews, T. M. Leslie, N. F. Borrelli, *ACS Nano* **2008**, *2*, 2206.
- [23] R. Debnath, J. Tang, D. A. Barkhouse, X. Wang, A. G. Pattantyus-Abraham, L. Brzozowski, L. Levina, E. H. Sargent, *J. Am. Chem. Soc.* **2010**, *132*, 5952.
- [24] J. M. Luther, J. Gao, M. T. Lloyd, O. E. Semonin, M. C. Beard, A. J. Nozik, *Adv. Mater.* **2010**, *22*, 3704.
- [25] L. J. Diguna, Q. Shen, J. Kobayashi, T. Toyoda, *Appl. Phys. Lett.* **2007**, *91*, 023116.
- [26] A. G. Pattantyus-Abraham, I. J. Kramer, A. R. Barkhouse, X. Wang, G. Konstantatos, R. Debnath, L. Levina, I. Raabe, M. K. Nazeeruddin, M. Grätzel, E. H. Sargent, *ACS Nano* **2010**, *4*, 3374.
- [27] H. Liu, J. Tang, I. J. Kramer, R. Debnath, G. I. Koleilat, X. Wang, A. Fisher, R. Li, L. Brzozowski, L. Levina, E. H. Sargent, *Adv. Mater.* **2011**, *23*, 3832.
- [28] J. Gao, J. M. Luther, O. E. Semonin, R. J. Ellingson, A. J. Nozik, M. C. Beard, *Nano Lett.* **2011**, *11*, 1002.
- [29] J. Gao, C. L. Perkins, J. M. Luther, M. C. Hanna, H.-Y. Chen, O. E. Semonin, A. J. Nozik, R. J. Ellingson, M. C. Beard, *Nano Lett.* **2011**, *11*, 3263.
- [30] D. A. R. Barkhouse, R. Debnath, I. J. Kramer, D. Zhitomirsky, A. G. Pattantyus-Abraham, L. Levina, L. Etgar, M. Grätzel, E. H. Sargent, *Adv. Mater.* **2011**, *23*, 3134.
- [31] X. Wang, G. I. Koleilat, J. Tang, H. Liu, I. J. Kramer, R. Debnath, L. Brzozowski, D. A. R. Barkhouse, L. Levina, S. Hoogland, E. H. Sargent, *Nat. Photonics* **2011**, *5*, 480.
- [32] K. S. Leschkies, T. J. Beatty, M. S. Kang, D. J. Norris, E. S. Aydil, *ACS Nano* **2009**, *3*, 3638.
- [33] L. Etgar, W. Zhang, S. Gabriel, S. G. Hickey, M. K. Nazeeruddin, A. Eychmüller, B. Liu, M. Grätzel, *Adv. Mater.* **2012**, *24*, 2202.
- [34] L. Etgar, T. Moehl, S. Gabriel, S. G. Hickey, A. Eychmüller, M. Grätzel, *ACS Nano* **2012**, *6*, 3092.
- [35] Alexander H. Ip, Susanna M. Thon, Sjoerd Hoogland, Oleksandr Voznyy, David Zhitomirsky, Ratan Debnath, Larissa Levina, Lisa R. Rollny, Graham H. Carey, Armin Fischer, Kyle W. Kemp, Illan J. Kramer, Zhijun Ning, André J. Labelle, Kang Wei Chou, Aram Amassian & Edward H. Sargent, *Nature Nanotechnology* **2012**, *7*, 577–582.